

Simulation of the Quasi-Biennial Oscillations of the Zonal Wind in the Equatorial Stratosphere: Part I. Low-Parameter Models

D. V. Kulyamin, E. M. Volodin, and V. P. Dymnikov

Institute of Numerical Mathematics, Russian Academy of Sciences, ul. Gubkina 8, Moscow, 119991 Russia

e-mail: kulyamind@mail.ru

Received July 20, 2007; in final form, September 10, 2007

Abstract—The paper focuses on the simulation of the quasi-biennial oscillations (QBOs) of zonal velocity in the equatorial stratosphere. Low-parameter models are used to examine two mechanisms for excitation of the QBO: one through the interaction of planetary waves with the mean flow at critical levels and another through gravity-wave obliteration. The possible use of each of these mechanisms for generating the QBO is shown, the ranges of parameter values where this generation is possible are determined, and the dependences of the period and amplitude of the limit cycle on the model parameters are analyzed. A relative role of waves of different scales in the formation of the period of the oscillations of zonal wind is studied with a coupled model combining both mechanisms. The conditions that are required to reproduce the QBO in general circulation models are discussed.

DOI: 10.1134/S0001433808010027

INTRODUCTION

Since the 1960s, when early observations of the quasi-biennial oscillations (QBOs) of the zonal wind in the equatorial stratosphere emerged, the number of studies of different QBO aspects has been increasing continually. This global climatic phenomenon can be described as slow downward-propagating westerly and easterly phases of zonal wind alternating with a period of about 28 months (such oscillations are directly observed in the equatorial zone at heights between 16 and 50 km). Figure 1 shows the time–height plot of the zonal wind in the equatorial stratosphere from the NCEP data [1] for eight years. The figure graphically demonstrates the essence of this phenomenon (direction of zonally averaged wind in the stratosphere changes periodically) and its basic properties: a period varying from 24 to 30 months, slow downward propagation of differently directed velocity phases (the rate of downward propagation is 1 km/month on average), the zone of propagation (at 60 to 10 mb), and the amplitude of zonal velocity and its distribution (with maxima of about 30 m/s at 20 to 10 mb).

In a zonal direction, intense QBOs are observed in a narrow equatorial zone ($\approx 6^\circ$ northward and southward of the equator). The distribution of the amplitude of velocity oscillations is approximately symmetric about the equator and close to a normal distribution with a maximum at the equator [2].

A detailed present-day overview of all aspects of the QBO is given in [3].

Despite a seemingly meridional localization of this phenomenon, there is a large amount of information

on the influence of the QBO on global climatic characteristics. A major proposed mechanism of the effect of the QBO on atmospheric dynamics is associated with the modulation of wave-activity transport in the extratropical stratosphere (basically by stationary waves). This modulation can trigger sudden stratospheric warmings; however, analysis of observations shows that the connection of these events is ambiguous [3–5]. Modulation is also responsible for the interaction of the QBO with other low-frequency processes like El Niño, the basic manifestation of which shows up in the impact on the amplitudes of planetary waves in the troposphere [3, 6, 7]. Analysis of observational data reveals the influence of the annual insolation forcing on the QBO and the nonlinear synchronization of the quasi-biennial and annual cycles [3, 8, 9].

It is also worth noting regional connections of the QBO with tropical processes, for example, with the duration of seasonal rains in the tropics and with the activity of tropical hurricanes in the Atlantic [10].

Since the QBOs of zonal wind are directly related to analogous oscillations of tropical stratospheric temperature, the influence of the QBO on the production of ozone and its transport toward the poles (through the modulation of dynamic processes in the stratosphere) also seems logical [11–13]. Analogous tendencies were found in the transport of other atmospheric pollutants resulting from different anthropogenic impacts or volcanic activity [3, 14, 15]. The connection of the QBO with the carbon cycle in the atmosphere may also be of importance.

It should be noted that, in several studies [16–18], the QBO is treated in the context of the parametric res-

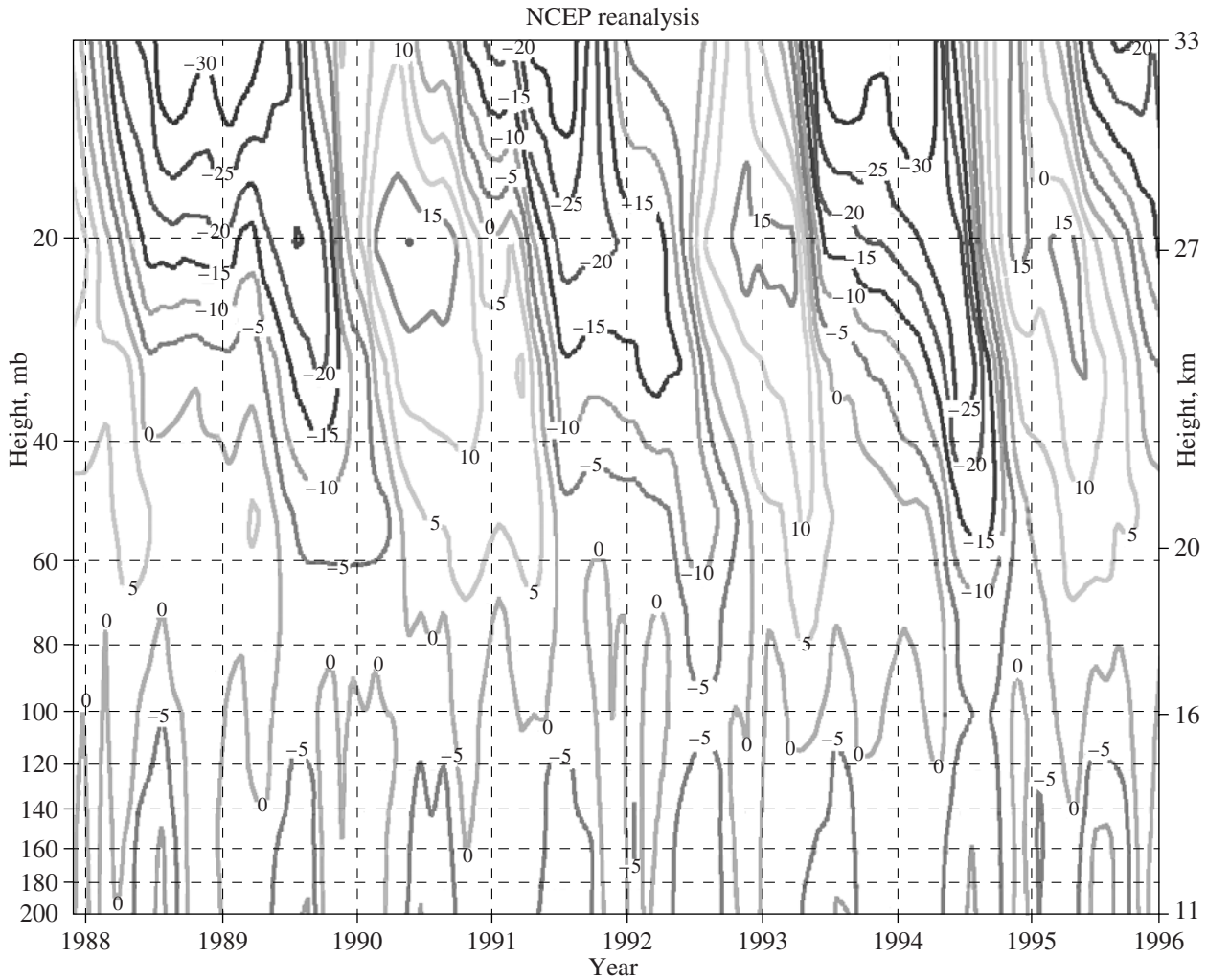


Fig. 1. Zonally averaged equatorial wind from the 8-year NCEP analysis in a height range from 200 to 10 mb. Velocity is given in m/s, the contour interval is 5 m/s, and dotted lines indicate westerly winds (negative direction).

onance effect; however, such an interpretation fails to explain some of the key features of the real quasi-biennial oscillations of zonal wind.

Despite the significance of the QBO, only few climate models are now able to reproduce this phenomenon [3, 19, 20]. In particular, the Max Planck Institute's MAECHAM5 model of high vertical resolution reproduces the QBO rather realistically [21]. This may be attributed to complicated and poorly understood mechanisms of the formation of this process. The explanation that the QBO of the zonal wind in the equatorial stratosphere arises from nonlinear interaction between the mean flow and equatorial waves propagating upward now appears to be well established.

Holton and Lindzen's pioneering research [22] showed that the main mechanism for this interaction can be planetary waves—mixed Rossby–gravity waves and Kelvin waves; however, it was found later

that the energy of these waves is obviously insufficient and that a full spectrum of equatorial waves should be considered down to the shortest gravity waves [3, 23]. While the mechanism for the interaction of planetary waves with the mean flow has already been clarified in earlier studies (this mechanism is based on the interaction of waves with the mean flow at critical levels where the phase speed of the waves is equal to that of the basic flow), the mechanism of the interaction of short gravity waves with the mean flow is still unclear [23, 24].

Since critical levels (or more precisely, critical layers) are narrow interaction zones, it is evident that an adequate simulation of the interaction requires that climate models be of high spatial (vertical) resolution, a necessary (yet insufficient!) condition for reproducing the QBO.

Since we assume that the type of interaction of short and long equatorial waves with the mean flow

can be different, we may conditionally divide all equatorial waves into two groups. The first group includes large-scale waves such as trapped equatorial Kelvin waves, mixed Rossby–gravity waves, and long inertia–gravity waves (with periods of about 1 to 5 days, zonal wavelengths over 1000 km). Another group includes small-scale gravity waves (with periods \ll 1 day and zonal wavelengths of 10 to 1000 km). As was noted above, despite a significant difference between these groups, their contribution to the total momentum transferred by them to the zonal flow is of almost equal importance [23].

Based on the above, we have attempted to answer the following questions in the first part of this study.

(1) The degree of the interaction of long equatorial waves with the mean flow, which is based on the interaction at critical levels, must evidently depend on a time and spatial resolution of an appropriate finite-dimensional approximation. Mathematically, any nonlinear model that adequately reproduces the QBO must generate a limit cycle with a period of about 2 years in a reasonable range of the model's parameters. As such, we can also use the parameters of the spatial and temporal approximation.

It is also interesting to discuss whether the generated limit cycle is a global attractor or if this attractor is local.

In this paper, the basic model for investigating the QBO arising from interaction of long waves with the zonal flow was the Plumb model [25], which will be described in Section 1 of this paper.

(2) Since the mechanism of wave interaction at critical levels could not be resolved in an atmospheric general circulation models of relatively coarse vertical resolution, the question arises of whether it might be possible to obtain the QBO using only a parametrization of the interaction of short gravity waves with the mean flow. The answer to this question, certainly, depends to a large extent on what method is used for parametrization. In our study, the model of the interaction of short gravity waves with the mean flow was that proposed by Hines [26, 27], which we have historically used for describing the interaction of gravity waves with the mean flow in the middle atmosphere. This method will be described in detail in the corresponding section; we only mention now that the problem lies in investigating the range of parameters of the model in which it must generate the limit cycle.

(3) With a positive answer to the previous question, the next problem is to study the relative role of equatorial waves of different scales in QBO formation. It is of interest to consider which waves determine the basic characteristics of the QBO of zonal velocity and what contribution comes from the other waves. To this end, the combined action of the QBO excitation mechanisms described above should be studied on the basis

of an extended model of the interaction of short and long waves with the mean flow.

This paper is the first part of a cycle consisting of two works. The second will be devoted to the simulation of the QBO in atmospheric general circulation models that are being developed at the Institute of Numerical Mathematics of the Russian Academy of Sciences.

1. SIMULATION OF THE QBO THROUGH INTERACTION OF LONG WAVES WITH THE MEAN FLOW

As was pointed out in the Introduction, the first mechanism for the excitation of the QBO is considered to be the interaction of long equatorial waves with the mean flow at critical levels (layers). The original model accepted here was that proposed by Plumb [25]. For consistency with our atmospheric general circulation model used below, some changes were introduced into the Plumb model and characteristic parameters close to those really observed in the atmosphere were employed.

Before considering the Plumb model, we conceptually describe a mechanism of change of the QBO phases when the zonal flow interacts with oppositely directed waves. Let the zonal velocity be positive at the initial time. Reaching a critical level, a wave with a positive phase speed transfers momentum to the zonal flow and accelerates it in the direction of the phase speed. Because of vertical mixing, the critical level descends until it reaches the lower level. At that time, a wave with the opposite phase speed penetrates the stratosphere and is absorbed at the upper levels (this absorption condition will be specified below), producing the flow's acceleration in the direction of the negative phase speed, after which this wave interacts with the mean flow at critical levels, as described above. The cycle then repeats.

We briefly describe the main assumptions used in the Plumb model. The interaction between the basic flow and long equatorial waves is described by the equations of a two-dimensional (x, z) viscous Boussinesq fluid in the gravity-force field with thermal cooling.

The two-dimensional structure of motion is described in terms of the stream function ψ with a vertical coordinate z and a horizontal coordinate x (in these quantities, the horizontal velocity component is

$$u = -\frac{\partial\psi}{\partial z}, \text{ and the vertical component is } w = \frac{\partial\psi}{\partial x}.$$

The following notation is introduced: $\sigma = -g\frac{\partial\rho}{\rho}$ is the

buoyancy, $N = \frac{g}{\rho}\frac{\partial\rho}{\partial z}$ is the buoyancy frequency, μ is

the coefficient of viscosity, and ν is the thermal coefficient of Newtonian cooling. In the given terms, the

motion can be described by the vorticity equation and by the equation for the buoyancy:

$$\begin{aligned} \frac{\partial}{\partial t}(\Delta\psi) + \frac{\partial\sigma}{\partial x} - \mu(\Delta^2\psi) &= J(\psi, \Delta\psi), \\ \frac{\partial\sigma}{\partial t} - N^2\frac{\partial\psi}{\partial x} + \nu\sigma &= J(\psi, \sigma). \end{aligned} \quad (1.1)$$

In this system, the Jacobian is defined as $J(\varphi_1, \varphi_2) = \frac{\partial\varphi_1}{\partial x}\frac{\partial\varphi_2}{\partial z} - \frac{\partial\varphi_1}{\partial z}\frac{\partial\varphi_2}{\partial x}$, and the Laplacian is $\Delta\varphi = \frac{\partial^2\varphi}{\partial x^2} + \frac{\partial^2\varphi}{\partial z^2}$. The motion is separated into the mean and fluctu-

ating components, i.e., $\psi = \bar{\psi} + \psi'$, where averaging is done over the horizontal coordinate (it is this component that determines the zonal flow).

Several geophysical approximations are made, on the basis of which the solution for the fluctuating component in (1.1) may be written in the form

$$\psi'_n = \text{Re}[\bar{\psi}_n e^{ik_n(x - c_n t)}]. \quad (1.2)$$

These solutions prescribe the wave spectrum, with wave numbers k_n and phase velocities \bar{c}_n (in the horizontal direction); the waves are assumed to propagate from a specified source upward. The amplitude obeys the equation

$$\begin{aligned} \frac{\partial^2\bar{\psi}_n}{\partial z^2} + \left\{ \frac{N^2[1 + i\nu/k_n(\bar{u} - c_n)]}{(\bar{u} - c_n)^2} \right. \\ \left. - k_n^2 \frac{\partial u^2 / \partial z^2}{(\bar{u} - c_n)} \right\} \bar{\psi}_n = 0. \end{aligned} \quad (1.3)$$

Solving (1.3) with the use of the WKB approximation, we obtain the height dependence of an averaged momentum flux transferred to the mean flow by one wave:

$$\begin{aligned} \bar{F}_n(z) &= \rho \langle \overline{u'_n w'_n} \rangle \\ &= \rho \bar{F}_n(0) \exp \left\{ -s \int_0^z \frac{N\nu}{k_n(\bar{u} - c_n)^2} dz' \right\}, \end{aligned} \quad (1.4)$$

where s is the sign of the vertical component of the group velocity (for our model, $s = +1$ because waves propagating upward are of interest here). This quantity determines the evolution of the zonally averaged velocity \bar{u} .

The role of Newtonian cooling in the interaction of waves with the zonal flow is very important because, in view of the noninteraction theorem [28], this interaction in an incompressible fluid at $\nu = 0$ is absent. From (1.4), the absorption of wave energy occurs mainly near a critical level, thereby imposing certain

limitations on the methods of computation of the wave-energy flux.

Thus, the basic equation to be used in computations is of the form

$$\frac{\partial\bar{u}}{\partial t} - \mu \frac{\partial\bar{u}^2}{\partial z^2} = -\frac{1}{\rho} \sum_n \frac{\partial\bar{F}_n}{\partial z}. \quad (1.5)$$

The inclusion of the vertical-diffusion term in Eq. (1.5) is absolutely necessary to remove singularities in the region of a critical level and, consequently, to lower it, and to eliminate a singularity at the lower boundary of the domain of interest. Clearly, the magnitude of this coefficient must also be a parameter that determines characteristics of the limit cycle of (1.5).

As in the Plumb model [25], two waves differing only in the directions of phase speed are used as a wave forcing. Wave parameters (wavelength, amplitude) in the investigation were varied within the limits observed for long equatorial waves [3, 28].

The problem was considered in the stratospheric region: the lower boundary was set at the tropopause level, a source of wave energy was placed at the same level, and the upper boundary was at the stratopause level (~55 km). The boundary condition at the top of the domain was the Neumann condition, i.e., a zero gradient of zonal velocity $\left. \frac{\partial u}{\partial z} \right|_{z_{\max}} = 0$, and the

Dirichlet condition $u|_{z_0} = 0$ was prescribed at the lower boundary.

The initial conditions in all experiments were realistic velocity profiles and a standard density profile, from which the buoyancy frequency was computed. The choice of the initial velocity profile was unimportant because the convergence of the solution to the limit cycle turned out to be very rapid. Therefore, it is possible to state that it was experimentally established for a given problem that the limit cycle in the region of selected parameters proved to be a local attractor.

This conclusion certainly applies to a difference approximation of the original problem described by Eq. (1.5), which was constructed on a regular grid, with the space derivatives approximated by central differences and the time derivative approximated by a Crank–Nicholson scheme. The dependence of the solution on the level of spatial resolution (Δz) was studied first. It was shown that the closeness of the solutions obtained was observed starting with $\Delta z \sim 500$ m; therefore, the basic experiments on the sensitivity of the period of the limit cycle to the variation in external parameters were conducted with a spatial resolution of $\Delta z = 500$ m. As an example, Fig. 2 shows the result of a numerical experiment with parameters the majority of which correspond to those really observed in the atmosphere: $c_1 = c_2 = 30$ m/s; $k_1 = k_2 = 7.85 \times 10^{-7}$ m⁻¹; $F_1(0) = -F_2(0) = 2 \times 10^{-2}$ m²/s²; $\nu = 10^{-6}$ s⁻¹; $\mu = 0.3$ m²/s.

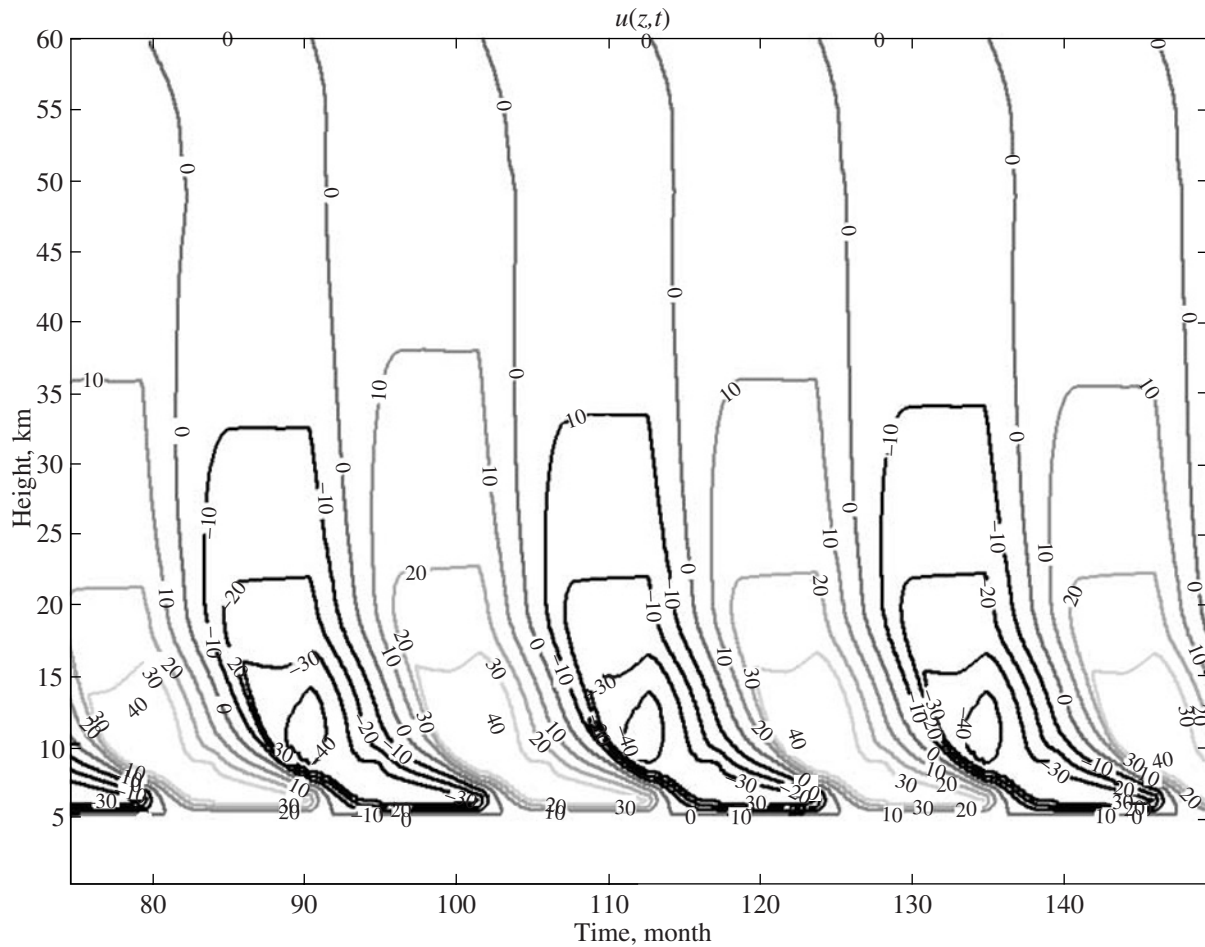


Fig. 2. Zonal-velocity profile close to the QBO, obtained from a numerical solution of the Plumb model (1.4) and Eq. (1.5) with realistic wave parameters. Velocity is given in m/s, the contour interval is 10 m/s, and dark contours correspond to the westerly wind phase (negative direction).

It should be noted that the amplitudes of the wave-energy source $F(0)$ in this experiment are well overestimated relative to the real ones in the atmosphere (in [25], Plumb, relying on Holton's research, offered a value of about $8 \times 10^{-3} \text{ m}^2/\text{s}^2$ for a Kelvin wave). With such a value of $F(0)$, the limit cycle is not excited. This result confirms the finding of earlier studies [23] that long waves by themselves possess no sufficient energy to produce the QBO.

Further studies of Eq. (1.5) were concerned with an investigation of the dependence of the period of the limit cycle on the key parameters of the problem (in our opinion, this problem has not received sufficient attention in the cited works). From a large number of experiments, it was found that a general dependence of the limit cycle on parameters of the problem can be written as

$$T \sim \frac{kc}{F_0}. \quad (1.6)$$

However, it is worth noting that the range of values of the parameters $F(0)$ and μ in which the solution had the form of a limit cycle with such a dependence of the period is relatively small, and this circumstance means that the characteristics of the QBO are very sensitive to the variation of these parameters. A fairly large number of experiments were conducted in which strictly linear dependences on k and c were obtained in a relatively broad range of their variation ($2\pi/(4 \times 10^7) \text{ m}^{-1} < k < 2\pi/(5 \times 10^6) \text{ m}^{-1}$; $15 \text{ m s}^{-1} < c < 45 \text{ m s}^{-1}$) (see Figs. 3b, 3c). This region corresponds to long equatorial waves and to their parameters comparable with their real values [3, 28]. As for $F(0)$, there is a rather nontrivial dependence of the period on this parameter (Fig. 3a). Note that dependence (1.6) was obtained for the minimum possible values of $F(0)$ at which the limit cycle still arises. For superlarge $F(0)$ values, the physics of formation of the limit-cycle period at small μ will already be governed by the time of a diffusion process within which velocities close to the phase speed of the wave will be established at a given height. Therefore, the dependence of the period on the initial

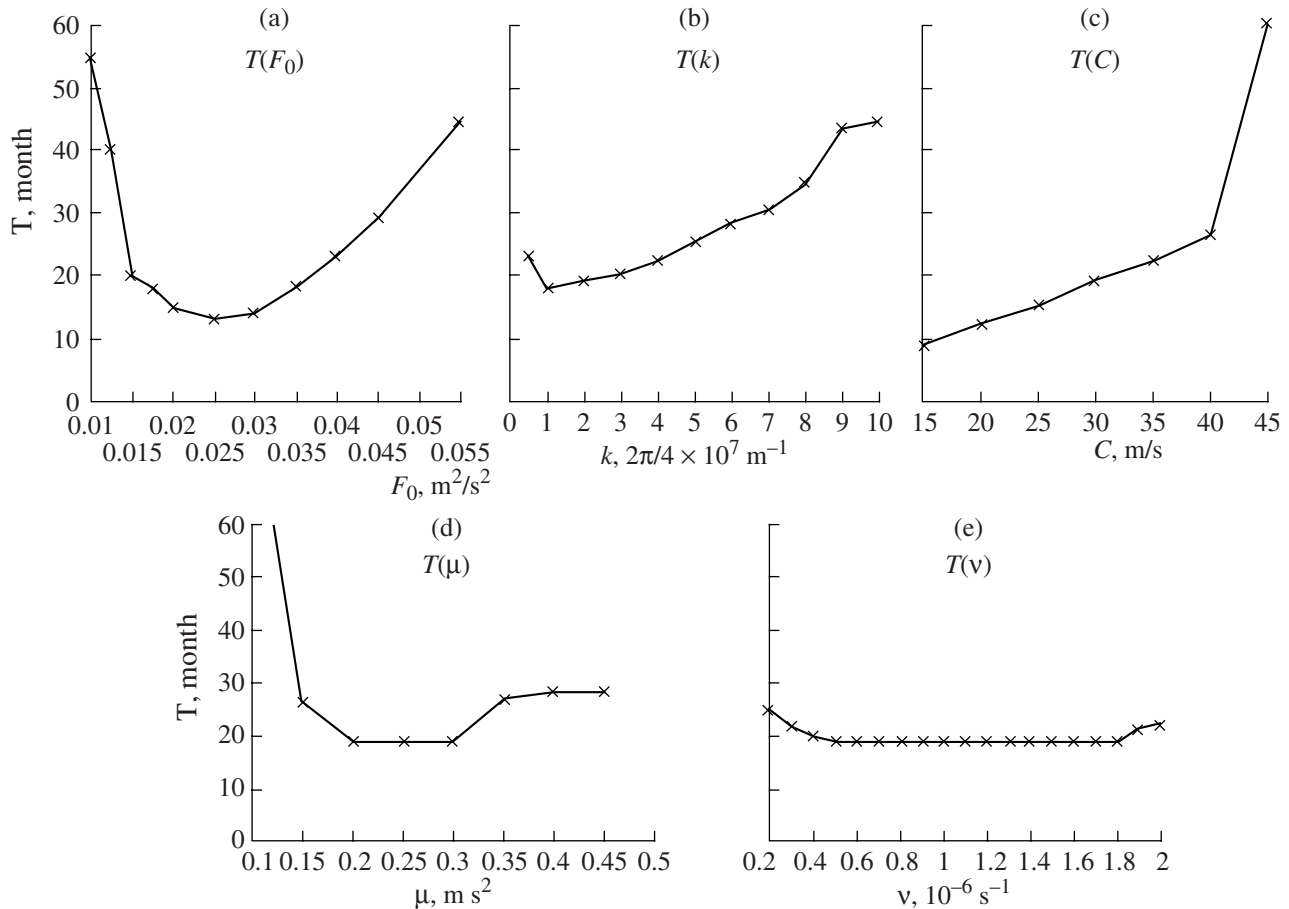


Fig. 3. Period of zonal-velocity oscillations as a function of (a) the initial wave momentum flux, (b) horizontal wave number, (c) phase speed, (d) diffusion coefficient, and (e) thermal dissipation coefficient from numerical experiments with the Plumb model (1.4) and Eq. (1.5) with symmetric waves.

$F(0)$ will be inverse. However, this case has little bearing on reality and is of interest only from a mathematical point of view on the study of problem (1.5).

For the diffusion coefficient μ , the QBO is obtained in a narrow range ($0.2 \text{ m}^2/\text{s} < \mu < 0.3 \text{ m}^2/\text{s}$), and the period in this range is independent of its value (Fig. 3d). As for the thermal dissipation coefficient ν , the period varies hardly at all over a broad range of its values (Fig. 3e).

It is worth noting that the period and amplitude of the oscillations obtained in a simulation of the interaction of long waves with the zonal flow are in proportional dependence, which agrees with the results of analysis of the actual QBO data [29].

Since one of the basic problems formulated in the Introduction is to examine the generation of the QBO by waves of different ranges, it is important to understand which of the key parameters of these waves are responsible for the period and amplitude of the QBO. Within the framework of the problem of wave–mean flow interaction at critical levels, this can be done by considering not two but more planetary waves as forc-

ing. For this purpose, another two oppositely directed symmetric waves with a smaller initial momentum but with a higher horizontal wave number were added to the wave forcing. As a result, zonal-velocity oscillations with the period controlled by waves with a larger initial momentum flux were obtained. The other waves contributed to the amplitude of zonal velocity and its vertical distribution. In a real atmosphere, a significant portion of the initial momentum flux is accounted for by a Kelvin wave and a mixed Rossby–gravity wave, which determine the duration of the QBO phases. Being absorbed by the mean flow at higher levels, shorter waves carry a smaller flux and maintain the QBO up to the upper levels of the stratosphere.

2. SIMULATION OF THE QBO THROUGH GRAVITY-WAVE OBLITERATION

The interaction of small-scale gravity waves with the background flow is rather difficult to treat on the same basis as the interaction with long waves at critical levels. One must turn to small scales and take into

account the statistical character of small-scale disturbances and the presence of an actually continuous spectrum of vertically propagating gravity waves, which transfer momentum and energy to the mean flow, interacting with each other. In general circulation models, this is a subgrid-scale process, and the interaction problem is solved in modern climate models with parametrizations of gravity-wave drag.

One of the recent parametrizations of this process has been developed by K. Hines and is being used in many general circulation models (for a detailed description, see [26, 27]). This parametrization is based on the theory of the Doppler shift of the middle portion of the spectrum of gravity waves toward higher vertical wave numbers, at which wave obliteration and momentum and energy transfer to the mean flow occur. This parametrization is of a semiempirical nature because part of the characteristics essential to a theoretical consideration is derived from statistical data processing.

A study of the mechanism of excitation of zonal-velocity oscillations by gravity-wave drag is carried out with a simple one-dimensional model analogous to that considered in Section 1. Since all distinctions between these two mechanisms lie in the definition of wave forcing, vertical diffusion is the necessary process for the implementation of a scheme of direction change. For the process of gravity-wave obliteration, this conclusion is not as evident as before, but it is supported by numerous numerical experiments. Following the same arguments as those used for the Plumb model, we write a one-dimensional equation for the evolution of the zonally averaged velocity component at the equator with the same notation:

$$\frac{\partial u}{\partial t} - \mu \frac{\partial^2 u}{\partial z^2} = -\frac{1}{\rho} \frac{\partial F_{\text{Hines}}}{\partial z}. \quad (2.1)$$

In Eq. (2.1), the right-hand side F_{Hines} denotes the momentum flux from wave obliteration, which will be calculated following the ideas suggested by Hines [26].

In a theoretical derivation of the gravity-wave propagation process, we will consider an elementary dispersion relation for an individual wave, which is based on the assumption of isotropy of its velocity:

$$Nm^{-1} = \Omega h^{-1}. \quad (2.2)$$

In (2.2), $N = -\frac{g}{\rho} \frac{\partial \rho}{\partial z}$ is the buoyancy frequency (ρ is the density of air at a given height, z is the vertical coordinate, and g is the acceleration of gravity); Ω is the gravity-wave frequency in a reference frame moving with the mean flow; and m and h are vertical and horizontal wave numbers, respectively. Hines proposed to treat the Doppler shift for each individual element of the wave spectrum by using a vertical wave

number at the source level as a marker (we denote it by m_i). Such a treatment makes it possible to determine the Doppler shift by statistical techniques, specifying a vertical-wave-number spectrum at the source level. For the sake of convenience, the vertical spectrum at this level is considered to be linear. Thus, based on this dispersion relation and on the assumption that the horizontal wave number does not vary with height, we can write a standard equation for the Doppler effect in passing to a reference frame moving with the Earth (in this frame, the frequency ω does not depend on height because it is a characteristic of an individual wave):

$$\omega h^{-1} = \Omega h^{-1} + V = Nm^{-1} + V. \quad (2.3)$$

In (2.3), V is the background horizontal velocity of airflow in the given direction (the vertical component of wind is assumed to be small and, therefore, is neglected). The background flow is taken to be a superposition of the mean flow and wave disturbances; i.e., $V = u + v$ for each direction and height. Since the left-hand side of (2.3) with the accepted assumptions is independent of height, we can write it for the level of the source of gravity waves at which the vertical spectrum is specified, the initial wave-induced fluctuation of the horizontal flow being neglected:

$$N(z_0)m_i^{-1} + \bar{u}(z_0) = N(z)m^{-1} + u(z) + v(z). \quad (2.4)$$

In the given equation, the quantities are isolated that depend on the vertical coordinate z , the value of which at the source level is denoted through z_0 . Expression (2.4) prescribes the Doppler shift in the spectrum of vertical wave numbers for any element of interest in the initial spectrum; it is the key equation for the given parametrization. Variations in the vertical wave numbers lead to a shift toward larger wave numbers because, for each element of the initial spectrum at any given height, a critical value exists at which the wave breaks down. From the theory of propagation of gravity waves in the atmosphere, it is known that fluctuations in the vertical plane in the flow cannot occur with a frequency higher than the buoyancy frequency N . Hence, the condition of nonobliteration of gravity waves results, which can be written for a characteristic disturbed velocity in the following form:

$$\frac{\partial v}{\partial z} < N. \quad (2.5)$$

As was noted above, we are dealing with a broad spectrum of gravity waves, the amplitude of which is normally distributed with zero mean and the height-dependent variance σ . Assuming that the amplitude is equal in order of magnitude to the rms deviation v , we can write the condition of nonobliteration as

$$\Phi_1 \sigma m < N, \quad (2.6)$$

where Φ_1 is the first of several statistical dimensionless factors introduced by the author. The recommended range of its values is $0.1 < \Phi_1 < 0.4$ (see [26]).

Thus, condition (2.6) yields a critical maximum limit value of vertical wave number m_{\max} , which for any height is determined as

$$m_{\max} = \frac{N(z)}{\Phi_1 \sigma(z)}. \quad (2.7)$$

Equation (2.7) for the limit vertical wave number, in combination with Eq. (2.4) for the Doppler shift of each separate portion of the initial spectrum in height, provides necessary conditions for the value of critical heights for any initial-spectrum element m_i :

$$m_{iC} = N(z_0) [\Phi_1 \sigma + u(z) - u(z_0) + v(z)]^{-1}. \quad (2.8)$$

The value $m_{iC}(z)$ for any height identifies the maximum wave number of the initial spectrum where the wave is not yet obliterated at this level: waves with vertical wave numbers $m_i < m_{iC}(z)$ propagate above the level z , and waves from the initial spectrum with $m_i \geq m_{iC}(z)$ are obliterated or were obliterated earlier.

For $v(z)$, Hines [26] proposed another empirical relation, based on observational data processing:

$$v(z) = \Phi_2 \hat{\sigma}(z). \quad (2.9)$$

Here, Φ_2 is a second statistical dimensionless parameter on the order of unity and $\hat{\sigma}(z)$ is the rms deviation in a given direction.

For computation of $F_{\text{Hines}} = \overline{\rho v w}$ in any direction (where v and w are the horizontal and vertical components of wave disturbances), it is accepted that vertical disturbances are in phase with horizontal ones, i.e., $v h = m w$. For each element of a continuous spectrum, the vertical flux of horizontal momentum is taken to be conserved until the obliteration of the wave occurs, and so it is possible to write an expression for the total flux across the entire spectrum in a given direction through the integral over the initial vertical spectrum:

$$\begin{aligned} F(z) &= \int_{m_{\min}}^{m_{\max}} \rho(z) \overline{v(z) w(z)} dm(z) \\ &= \int_{m_{i\min}}^{m_{iC}} \rho(z_0) \overline{v(z_0) w(z_0)} dm_i. \end{aligned} \quad (2.10)$$

Taking into account the fact that we ourselves specify the initial vertical spectrum, restricting it by the condition of wave nonobliteration (2.6) at the initial level, we will generally assume that the energy distribution is given by the function $P(m_i)$ within the interval $m_{i\min} \leq m_i \leq N(z_0) [\Phi_1 \sigma(z_0) + \Phi_2 \hat{\sigma}(z_0)]^{-1}$.

Expression (2.10), with consideration for the synchronization condition of disturbances, can then be rewritten as

$$\begin{aligned} F(z) &= \int_{m_{i\min}}^{m_{iC}} \rho(z_0) \overline{v(z_0) w(z_0)} h / m_i dm_i \\ &= \rho(z_0) \hat{\sigma}(z_0)^2 h \int_{m_{i\min}}^{m_{iC}} P(m_i) / m_i dm_i. \end{aligned} \quad (2.11)$$

The height distribution of critical values for vertical wave numbers in any direction is of the form

$$\begin{aligned} m_{iC}(\text{trial})^{\pm} \\ = N(z_0) [\Phi_1 \sigma(z) + \Phi_2 \sigma^{\pm}(z) \pm (u(z) - u(z_0))]^{-1}. \end{aligned} \quad (2.12)$$

In (2.12), $N(z_0)$ is the buoyancy frequency at the source level, Φ_1 and Φ_2 are dimensionless statistical parameters of about unity that are determined from data on wave activity, and $\sigma^+(z)$ and $\sigma^-(z)$ are the rms deviations in each of the directions, which are calculated in a system with these equations for any height by the following formulas:

$$\begin{aligned} \sigma^{\pm}(z)^2 &= \rho^{-1}(z) \rho(z_0) N(z) N(z_0)^{-1} \sigma^2(z_0) \\ &\times \int_{m_{i\min}}^{m_{iC}} C m_i [1 \mp N(z_0)^{-1} (u(z) - u(z_0)) m_i]^{-1} dm_i. \end{aligned} \quad (2.13)$$

Equations (2.13) are the integral formulas for the rms deviations, $m_{i\min}$ is the lower limit of the vertical wave number spectrum, the constant $C = 2(m_{i\max}^2 - m_{i\min}^2)^{-1}$ is determined by the linear spectrum and the normalization condition, and the upper limit $m_{i\max} = N(z_0) [(\sqrt{2} \Phi_1 + \Phi_2) \sigma(z_0)]^{-1}$ is the critical value of the wave spectrum at the source, determined by (2.12). The total variance for any level is calculated as $\sigma(z) = \sqrt{\sigma^+(z)^2 + \sigma^-(z)^2}$.

We note that (2.12) is not a final but a trial equation, because two factors must be taken into account: m_{iC}^{\pm} cannot increase with height because the waves propagating upward are obliterated down at a certain level and are not able to go up above this level; these quantities cannot be negative. A test of these conditions must be implemented in the course of a numerical run.

After solving the system of equations and testing the necessary conditions for a trial value, we can write

an expression for the fluxes in both directions and for the total flux:

$$F^+(z) = \rho(z_0)\sigma(z_0)^2 h C(m_{iC}^+ - m_{i\min}), \quad (2.14)$$

$$F^-(z) = \rho(z_0)\sigma(z_0)^2 h C(m_{iC}^+ - m_{i\max}).$$

$$\begin{aligned} F_{\text{Hines}}(z) &= F^+(z) - F^-(z) \\ &= \rho(z_0)\sigma(z_0)^2 h C(m_{iC}^+ - m_{iC}^-). \end{aligned} \quad (2.15)$$

To examine the evolution of velocity, it is necessary to construct a one-dimensional numerical model on the basis of Eq. (2.1), in which the momentum flux will be calculated from (2.15), with solving the system of equations (2.12) and (2.13) for each direction. For simplicity, the zonal velocity at the lower boundary (the level of the wave source) is taken to be zero: $u(z_0) = 0$. At the upper boundary, we also set $u(z_{\max}) = 0$.

We assume that the momentum flux is zero below and at the source level and satisfies the radiation condition at the upper boundary:

$$F_{\text{Hines}}(z)|_{z \leq z_0} = 0, \quad \left. \frac{\partial F_{\text{Hines}}(z)}{\partial z} \right|_{z = z_{\max}} = 0. \quad (2.16)$$

It should be noted that we conducted a series of experiments on varying initial conditions, boundary conditions, and conditions (2.16), and no significant changes were introduced into general modeling results by these variations. Since our goal was to find the solution in the form of a limit cycle, all the results were analyzed after the lapse of a sufficiently long time interval.

By analogy with Section 1, a numerical approximation of (2.1), (2.12), (2.13), and (2.15) is performed on a regular grid. A semi-implicit Crank–Nicholson-type scheme was used for time approximation, and a centered-difference scheme was employed for space approximation. Since the result must in principle depend little on resolution, we used a vertical grid with a resolution coinciding in the order of magnitude with vertical resolutions in state-of-the-art general circulation models. At each time step, we first calculate the vertical profile of the horizontal momentum flux $F_{\text{Hines}}(z)$ through the Hines parametrization from the vertical profile $u(z)$, which is already known. For this purpose, with consideration for a test of conditions, a system of finite-dimensional analogues of (2.12) and (2.13) is solved by iterations. The results obtained are then substituted into expression (2.15) for the flux, and the velocity profile $u(z)$ is then determined by a semi-implicit scheme from Eq. (2.1) for the next time step.

By analogy with the first part of this study, for a comprehensive analysis of the generated oscillations of mean velocity, a large number of experiments were conducted with the gravity-wave drag model under consideration. The main result of these experiments is that a parametrization of obliteration of short gravity

waves permits a solution in the form of a limit cycle with periods close to those of the QBO. The next problem was to calculate the range of the key parameters essentially determining this period.

The main characteristics that describe wave processes are the initial spectrum of vertical wave numbers and the amplitude distribution given by the rms deviation $\sigma(z_0)$. The vertical spectrum is assumed to be continuous and taken initially to be linear. Therefore, for vertical wave numbers, we can vary the spectrum limits at the source level. The horizontal wave spectrum in our case is taken to be unchanged with a constant wave number h . A series of experiments with different values of the horizontal wave number h and with different $\sigma(z_0)$ revealed some general tendencies. With increasing horizontal wave number, the oscillation period decreases proportionally, while the characteristic maximum amplitude of zonal velocity increases nonlinearly. The same occurs with increasing $\sigma(z_0)$, but the amplitude increases much faster, and the vertical structure of the cycle experiences no significant changes and remains symmetric about the change in velocity direction. A strong sensitivity of the oscillation characteristics to these parameters can also be seen.

A strong sensitivity of the generation mechanism of oscillations is found in a series of experiments on variation of vertical diffusivity. With increasing vertical diffusivity, the period and amplitude of oscillations decrease. When the vertical diffusivity approaches zero, the oscillations are no longer excited, an outcome that is indicative of the role of this process in the mechanism based on gravity-wave drag as well.

In our experiments, we can also vary the lower limit of the vertical wave spectrum at the source level, $m_{i\min}$. Physically, varying this quantity leads to a shift in the distribution of energy over the spectrum and to a change in the wave range considered. With increasing $m_{i\min}$, the spectrum shifts toward higher frequency disturbances, thereby implying that small-scale gravity-wave processes carry a larger portion of energy. Numerical experiments have shown that the oscillation period is inversely proportional to $m_{i\min}$. The maximum amplitude of zonal velocity in the observed oscillations decreases nonlinearly with an increase in the minimum wave number.

From the results of experiments, we can determine the dependence of the period of zonal-velocity oscillations on the key parameters in the following way:

$$T \sim \frac{1}{h\sigma_0^2 m_{i\min} \sqrt{\mu}}. \quad (2.17)$$

As an example, Fig. 4 shows the results of a computation of the oscillations of zonal velocity with the model described above, in which the following param-

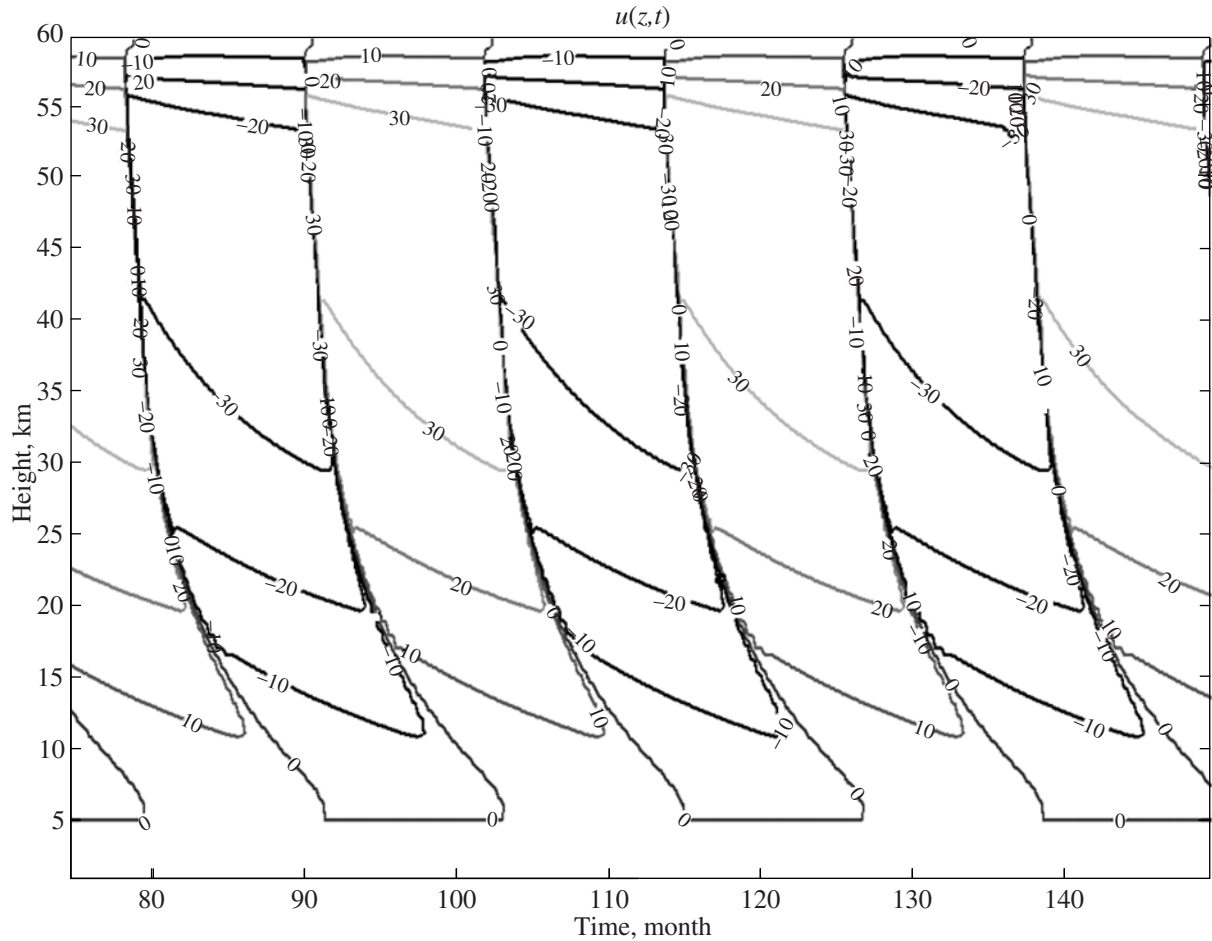


Fig. 4. Zonal-velocity profile close to the QBO obtained from a numerical solution of the Hines model (2.1) and (2.15). Velocity is given in m/s, the contour interval is 10 m/s, and dark contours correspond to the westerly wind phase (negative direction).

eters were taken: $\Phi_1 = 0.3$, $\Phi_2 = 1.5$, $\sigma_0^2 = 1 \text{ m}^{-2} \text{ s}^{-2}$, $m_{\min} = 10^{-4} \text{ m}^{-1}$, $\mu = 0.3 \text{ m s}^{-2}$, and $h = 10^{-5} \text{ m}^{-1}$. It is easy to see that, with the parameters thus selected, we obtain a situation close to the actually observed QBOs of zonal velocity in the equatorial stratosphere.

3. SIMULATION OF THE QBO THROUGH THE COMBINED INTERACTION OF GRAVITY AND PLANETARY WAVES WITH ZONAL FLOW

From the results of the previous sections, the study of the combined action of both mechanisms described above is of most interest. Since the proposed approaches with a certain choice of parameters span a full spectrum of equatorial waves, it is possible to describe the interaction of equatorial waves with the mean flow realistically in a generalized model and, on its basis, to attempt to obtain the QBO with the required characteristics. Since the methods for investigating the mechanisms of the interaction of long and

short gravity waves are based on similar one-dimensional models, an analogous coupled model was used to produce their combined action.

In accordance with the first section of this study, the system was assumed to comprise two large-scale waves propagating vertically, analogues of two long equatorial waves of different direction (Kelvin wave and Rossby-gravity wave). Following the Plumb model [25], we consider the interaction of these waves with the mean flow in a medium with thermal dissipation. It is also assumed that the dynamics of airflow is subjected to gravity-wave drag, which is generated by the obliteration of short waves in the upper atmosphere. According to the second section of this study, the influence of small-scale waves on the dynamics of the mean flow was described by the Hines parametrization [26, 27]. The action of both wave types is specified by an averaged flux of horizontal momentum transferred to the mean flow.

Thus, the equation for the evolution of an averaged component of zonal velocity is written as

$$\frac{\partial \bar{u}}{\partial t} - \mu \frac{\partial \bar{u}^2}{\partial z^2} = -\frac{1}{\rho} \frac{\partial (F_{\text{Plumb}} + F_{\text{Hines}})}{\partial z}. \quad (3.1)$$

Here, the quantities F_{Plumb} and F_{Hines} specify the momentum fluxes produced by the interaction between the mean flow and long and short gravity waves, respectively. With (1.4) and (2.15), these fluxes can be written as

$$F_{\text{Plumb}}(z) = \rho(z) \sum_n F_n(z_0) \times \exp \left\{ -\int_0^z \frac{N(z') \nu}{k_n (\bar{u}(z') - c_n)^2} dz' \right\}, \quad (3.2)$$

$$F_{\text{Hines}}(z) = \rho(z_0) \sigma(z_0)^2 h C (m_{iC}^+(z) - m_{iC}^-(z)). \quad (3.3)$$

The quantities $m_{iC}^+(z)$ and $m_{iC}^-(z)$ are calculated by the method described in Section 2.

Equations (3.1)–(3.3) are the basic equations for describing the interaction of equatorial waves with the mean flow, which were used to examine the excitation of a QBO analogue in the presence of both mechanisms considered above. In a numerical solution of (3.1)–(3.3), a range of z from 0 to 60 km was considered and the source level z_0 was taken identical for both wave types in accordance with observed data, because both types of waves originate in the upper troposphere at about 8 km. A standard exponential density profile was specified, from which the buoyancy frequency was computed.

For simplicity, the zonal velocity at the wave-source level is taken to be zero: $u(z_0) = 0$. At the upper boundary, we also assume $u(60) = 0$. In accordance with the models developed, the flux of gravity waves below the source level is also set equal to zero. At the top of the atmosphere, the condition of complete absorption is assumed, $F_{\text{Hines}}(60) = 0$; that is, the waves are not emitted or reflected at the boundary.

Any realistic vertical profile of the vertical velocity can be chosen as initial conditions, because the system's solution then reduces to a limit cycle. However, in the given case where two different mechanisms operate, the system can take much more time to attain a steady state than in the case of each individual model. A piecewise linear velocity profile was used as the initial condition in all experiments.

A difference approximation was constructed on a regular grid, both in time and space. In accordance with the results from the Plumb model, a sufficiently high vertical resolution was used in all experiments to resolve interaction at critical levels (spacing 0.5 km). A semi-implicit Crank–Nicholson-type scheme was used for time approximation, and space approxima-

tion was performed with a centered-difference scheme of the second order of accuracy. At each time step, Eqs. (3.2) and (3.3) were solved separately via standard quadrature formulas to determine the momentum fluxes from each type of waves, and then the velocity evolution was computed from (3.1).

Analyzing the modeling results for each wave type from the previous sections, it can be concluded that the main interaction of long equatorial waves with the zonal flow occurs in the lower layers of the stratosphere. Therefore, the maximum amplitude of oscillations generated by this mechanism is in the lower stratosphere. The larger the horizontal wave number (i.e., the smaller the wave scale), the higher the level of this maximum. As for the mechanism of obliteration of gravity waves, its major effect on the zonal flow occurs in the upper stratosphere. We recall that Hines has developed a parametrization of gravity-wave drag for the stratosphere and mesosphere. For this reason, oscillations of zonal velocity generated by short gravity waves have maximum amplitudes in the upper layers.

Figure 5 shows the results of the experiment in which the initial momentum flux for long waves was taken close to the real one (recall that this quantity is not sufficient to produce the QBO); parameters of gravity waves were chosen the same as those for which an analogue of the QBO was derived in Section 2. As can be seen, the interaction of long waves with the mean flow performs its cycle in the lower layers. In this case, a redistribution of the flux from gravity waves occurs, because the mean velocity profile changes. The mechanism of excitation of the oscillations by gravity-wave drag also takes place, but it adjusts to oscillations in the lower layers. This result is confirmed by a series of other numerical experiments with different model parameters. In the given case, the oscillations in the upper stratosphere are modulated by oscillations in the lower layers.

By increasing the horizontal wave number for long waves, it is possible to make the regions of operation of both mechanisms coincident with each other. The result of a numerical experiment in which a steady profile of the oscillation was established is shown in Fig. 6. With the same parameters, the model with gravity waves alone produced a slightly larger oscillation period. For a clear demonstration of the long-wave-produced modulation of the oscillations generated by short gravity waves, Fig. 7 displays a result of the numerical experiment with more realistic asymmetric characteristics of long waves, where the phase speed of the easterly wave was greater, but characteristics of gravity waves remained symmetric. It is easy to see that a general steady asymmetric profile of oscillations was established. Based on the results of the experiments conducted with different wave types, it can be concluded that the asymmetric variable struc-

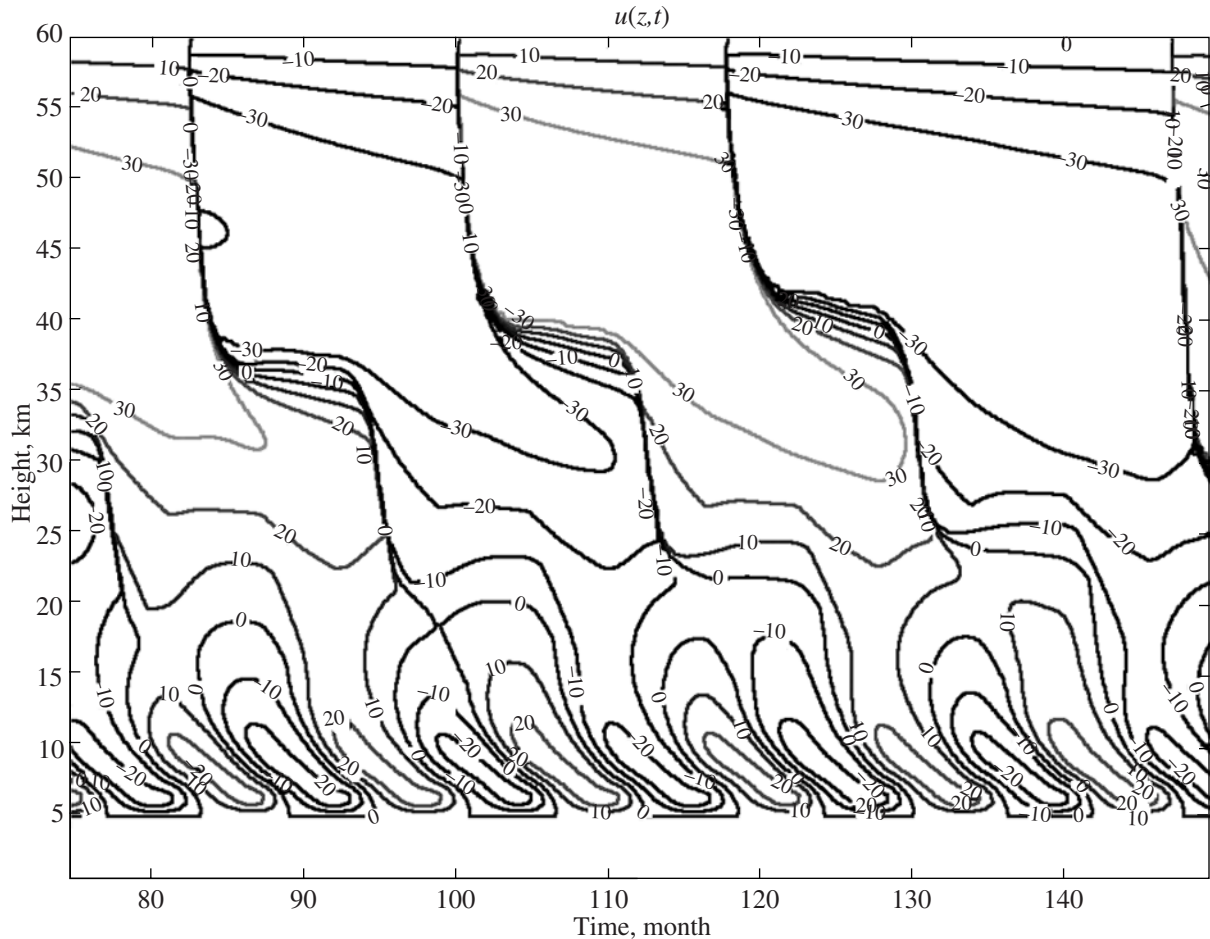


Fig. 5. Zonal-velocity profile obtained from a numerical solution of combined model (3.1). Velocity is given in m/s, the contour interval is 10 m/s, and dark contours correspond to the westerly wind phase (negative direction).

ture of the QBO at different heights is caused by long waves that deposit maximum momentum flux in these zones.

It can also be concluded that gravity waves play a secondary role in the formation of the QBO period, supplying sufficient momentum for its occurrence in the upper layers. Similar assumptions have been encountered in earlier studies (see [3]).

CONCLUSIONS

As was noted in the Introduction, very few of current atmospheric general circulation models reproduce the QBO of the zonal wind in the equatorial stratosphere, and it remains unclear what necessary and sufficient conditions the model must satisfy for the QBO to be reproduced. It is this problem that constitutes the main goal of this study. From the results of our study, the following conclusions can be drawn.

(1) An adequate simulation of the interaction of long planetary equatorial waves with the zonal flow at critical levels in the equatorial stratosphere requires a

high spatial resolution (<500 m in the vertical). We have examined how the period and amplitude of the oscillations of zonal wind depend on key parameters—horizontal wave numbers and phase velocities, Newtonian cooling rate and vertical diffusivity, and energy of the source of long waves. It is worth noting that these dependences should be treated as qualitative rather than quantitative ones because they were obtained with a relatively simple model; however, since nearly all of the above parameters of the atmospheric general circulation model are internal, their analysis is an important diagnostic problem.

(2) The results of this study as well as of earlier studies [3, 23] show that the level of energy of planetary waves alone is insufficient to excite the QBO of the zonal wind in the equatorial stratosphere. Therefore, it can be concluded that the full spectrum of equatorial waves participates in the formation of the QBO in some way or another. In this study, we have attempted to reproduce the QBO using the interaction of gravity waves with the zonal flow through the mechanism of obliteration. The model of gravity-

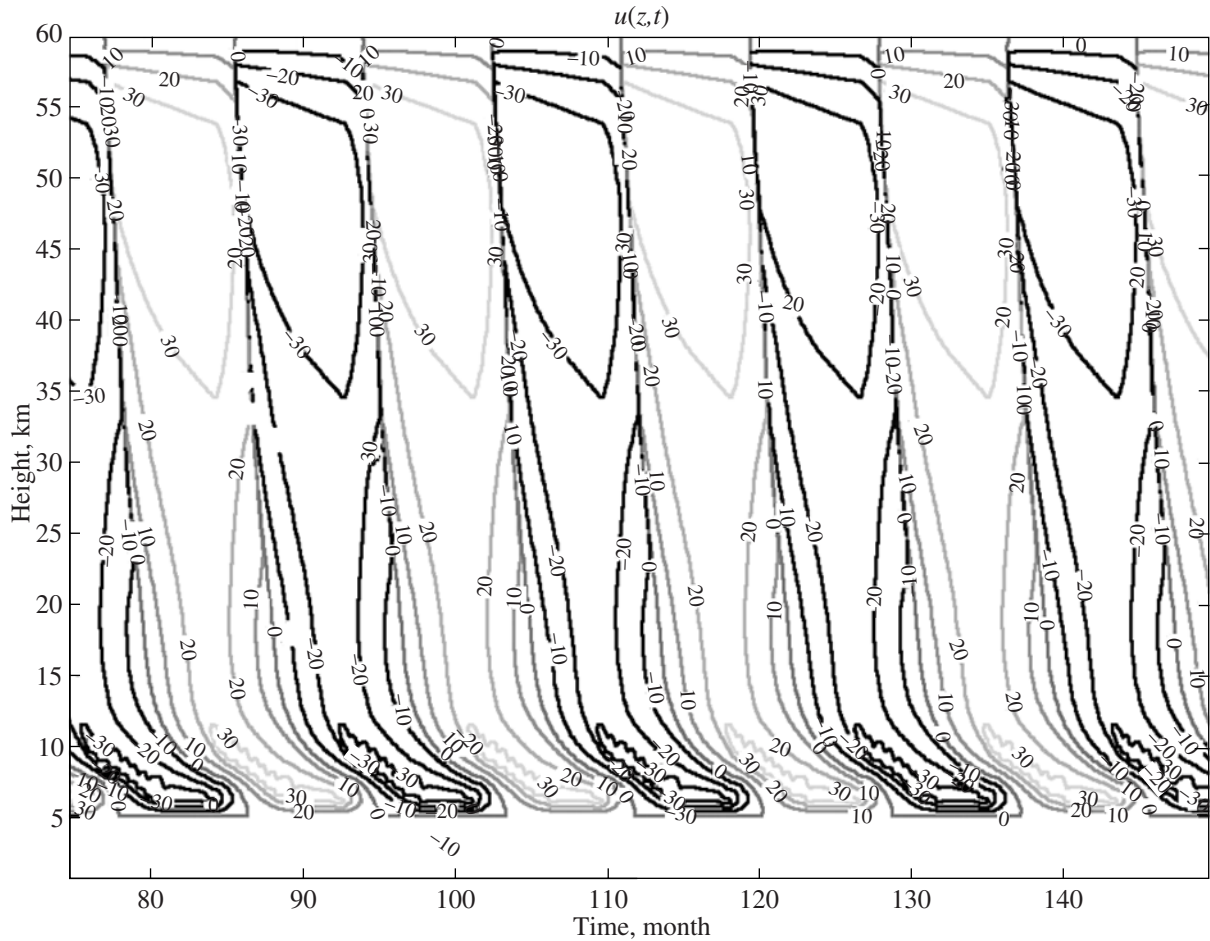


Fig. 6. Zonal-velocity profile from a numerical solution of combined model (3.1) with the same parameters as in Fig. 5, but with a horizontal wave number that is an order of magnitude larger for long waves. Velocity is in m/s, the contour interval is 10 m/s, and dark contours correspond to the westerly wind phase (negative direction).

wave generation and obliteration used here was proposed by Hines [26, 27]. The central result of this part of the study is the statement that the obliteration mechanism for short gravity waves is by itself sufficient for the excitation of the oscillations of the zonal equatorial wind. However, the relationships found between the period and amplitude of zonal-velocity oscillations and basic parameters of the model have shown that a pattern similar to the real QBO can be obtained only in a very narrow range of these parameters, thus casting into doubt the conclusion that this mechanism plays a key role in the generation of the QBO with realistic characteristics (this also applies to the problem of simulation of the QBO with atmospheric general circulation models).

(3) A more realistic picture is obtained if two wave sources are combined: a source due to planetary waves and short gravity waves. It should be noted, however, that most of the absorption of planetary waves takes place in the lower stratosphere, while the absorption

of gravity waves occurs in the upper stratosphere. An important result obtained in this study is that planetary waves play a key role in the period and asymmetry of the easterly and westerly phases of the QBO, while gravity waves have a secondary role, supplying the energy deficit to an oscillatory system. There seems to be some mechanism of synchronization of the two systems; however, this assumption calls for further detailed investigation.

In the MAECHAM5 model [21], in particular, realistic characteristics of the QBO were obtained at a high vertical resolution and at underestimated frequencies of gravity waves in the Hines parametrization, in agreement with the results of this work, but the reasons why the given model is able to reproduce the QBO have not been described so far.

We also mention that ascending vertical movements play a very important role in the generation of oscillations of zonal wind in the equatorial stratosphere. It was experimentally demonstrated that if the

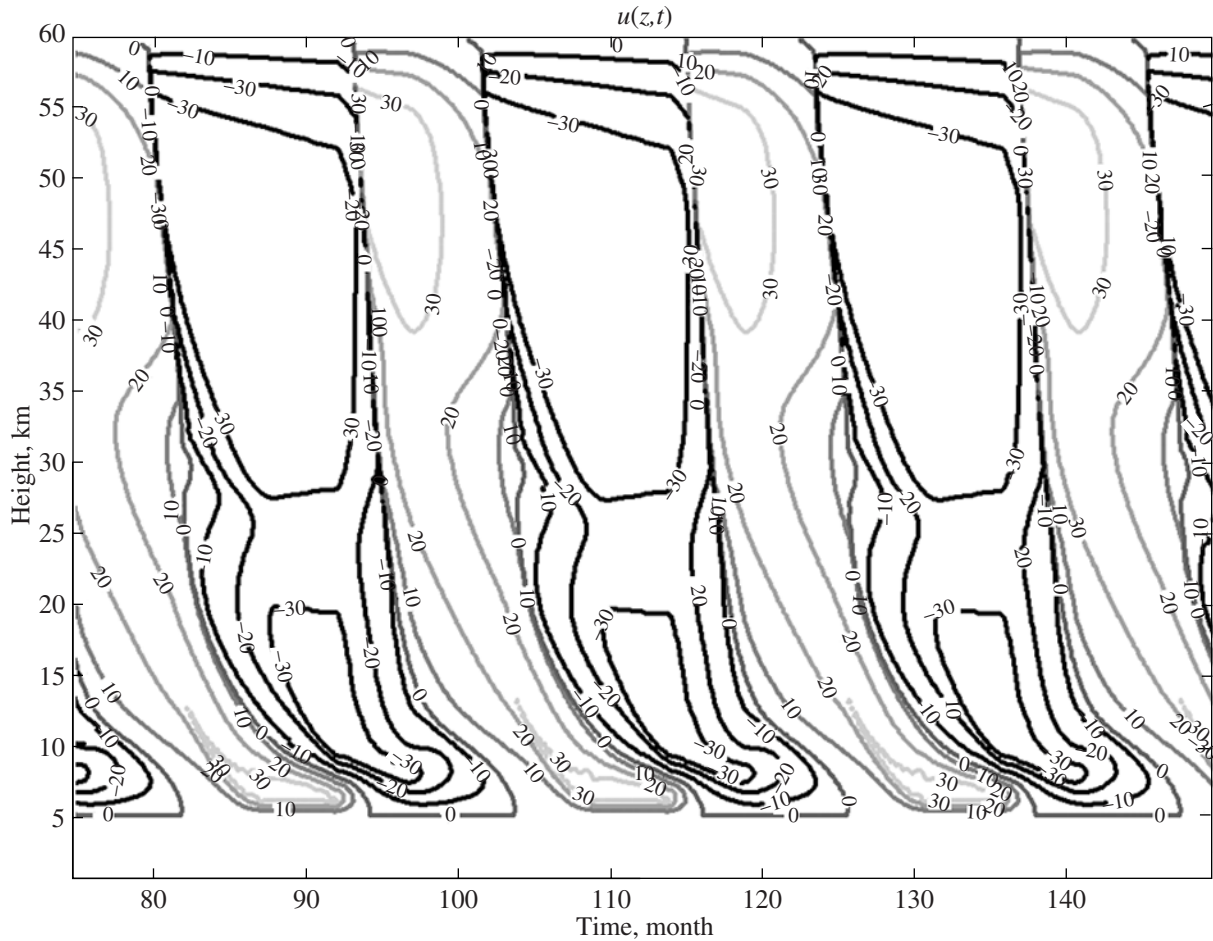


Fig. 7. Zonal-velocity profile from a numerical solution of (3.1) with the same parameters as in Fig. 6, but asymmetric phase velocities and wave numbers of long waves. Velocity is in m/s, the contour interval is 10 m/s, and dark contours correspond to the westerly phase (negative direction).

ascending movements are close in order of magnitude to the rate of change of the descending QBO phase, the limit cycle in the system disappears. (Results of these experiments have not been shown because of their relative obviousness.)

It follows from the results obtained that, with a relatively coarse vertical resolution of the atmospheric general circulation model, it is in principle possible to reproduce oscillations of the zonal wind in the equatorial stratosphere (without any description of the interaction of planetary waves with the zonal flow). However, characteristics of these oscillations are unlikely to be close to reality. Under conditions of real vertical movements at the equator and additional horizontal energy dissipation, the required energy of gravity waves to be parameterized must be high, and the period of the oscillations will, in fact, be shorter than two years.

REFERENCES

1. R. Kistler, et al., "The NCEP/NCAR 50-Year Reanalysis: Monthly Means CD-ROM and Documentation," *Bull. Am. Meteorol. Soc.* **82**, 247–266 (2001).
2. P. H. Haynes, "The Latitudinal Structure of the Quasi-Biennial Oscillation," *Q. J. R. Meteorol. Soc.* **124**, 2645–2670 (1998).
3. M. P. Baldwin, et al., "The Quasi-Biennial Oscillation," *Rev. Geophys.* **39**, 179–229 (2001).
4. J. R. Holton and H. C. Tan, "The Influence of the Equatorial Quasi-Biennial Oscillation on the Global Atmospheric Circulation at 50 mb," *J. Atmos. Sci.* **37**, 2200–2208.
5. T. J. Dunkerton and M. P. Baldwin, "Quasi-Biennial Modulation of Planetary-Wave Fluxes in the Northern Hemisphere Winter," *J. Atmos. Sci.* **48**, 1043–1061 (1991).
6. W. M. Gray, J. D. Sheaffer, and J. A. Knaff, "Influence of the Stratospheric QBO on ENSO Variability," *J. Meteorol. Soc. Jpn.* **70**, 975–995 (1992).

7. M. P. Baldwin and T. J. Dunkerton, "Quasi-Biennial Modulations of the Southern Hemisphere Stratospheric Polar Vortex," *Geophys. Res. Lett.* **25**, 3343–3346 (1998).
8. A. N. Gruzdev and V. A. Bezverkhni, "Long-Term Variations in the Quasi-Biennial Oscillation of the Equatorial Stratospheric Wind," *Izv. Akad. Nauk, Fiz. Atmos. Okeana* **35**, 773–785 (1999) [*Izv., Atmos. Ocean. Phys.* **35**, 700–711 (1999)].
9. T. J. Dunkerton, "Annual Variation of Deseasonalized Mean Flow Acceleration in the Equatorial Lower Stratosphere," *J. Meteorol. Soc. Jpn.* **68**, 499–508 (1990).
10. J. A. Knaff, "Evidence of a Stratospheric QBO Modulation of Tropical Convection," Paper No. 520 (Dept. of Atmospheric Science, Colorado State Univ., Fort Collins, 1993).
11. W. J. Randel, F. Wu, R. Swinbank, et al., "Global QBO Circulation Derived from UKMO Stratospheric Analyses," *J. Atmos. Sci.* **56**, 457–474 (1999).
12. J. R. Holton, P. H. Haynes, M. E. McIntire, et al., "Stratosphere-Troposphere Exchange," *Rev. Geophys.* **33**, 403–439 (1995).
13. W. J. Randel and J. B. Cobb, "Coherent Variations of Monthly Mean Column Ozone and Lower Stratospheric Temperature," *J. Geophys. Res. D* **99**, 5433–5447 (1994).
14. D. B. A. Jones, H. R. Schneider, and M. B. McElroy, "Effects of the Quasi-Biennial Oscillation on the Zonally Averaged Transport of Tracers," *J. Geophys. Res. D* **103**, 11235–11249 (1998).
15. C. R. Trepte and M. H. Hitchman, "Tropical Stratospheric Circulation Deduced from Satellite Aerosol Data," *Nature* **355**, 626–628 (1992).
16. V. S. Purganskii, "On the Motion of the Atmosphere in the Equatorial Latitudes," *Meteorol. Gidrol.*, No. 11, 3–13 (1965).
17. E. B. Gledzer and A. M. Oboukhov, "Quasi-Biennial Oscillation As a Parametric Phenomenon in the Climate System," *Izv. Akad. Nauk SSSR, Fiz. Atmos. Okeana* **18**, 1154–1158 (1982).
18. I. I. Mokhov, V. A. Bezverkhni, and A. V. Eliseev, "Atmospheric Temperature Quasi-Biennial Oscillation and Its Tendencies for Change," *Izv. Akad. Nauk, Fiz. Atmos. Okeana* **33**, 579–587 (1997) [*Izv., Atmos. Ocean. Phys.* **33**, 533–541 (1997)].
19. B. A. Boville and W. J. Randel, "Equatorial Waves in a Stratospheric GCM: Effects of Vertical Resolution," *J. Atmos. Sci.* **49**, 785–801 (1992).
20. Y. Hayashi and D. G. Golder, "Kelvin and Mixed Rossby-Gravity Waves Appearing in the GFDL "SKYHI" General Circulation Model and the FGGE Data Set: Implications for Their Generation Mechanism and Role in the QBO," *J. Meteorol. Soc. Jpn.* **72**, 901–935 (1994).
21. M. A. Giorgetta, et al., "Climatology and Forcing of the Quasi-Biennial Oscillation in the MAECHAM5 Model," *J. Clim.* **19**, 3882–1901 (2006).
22. J. R. Holton and R. S. Lindzen, "An Updated Theory for the Quasi-Biennial Cycle of the Tropical Stratosphere," *J. Atmos. Sci.* **29**, 1076–1080 (1972).
23. T. J. Dunkerton, "The Role of Gravity Waves in the Quasi-Biennial Oscillation," *J. Geophys. Res. D* **102**, 26053–26076 (1997).
24. T. J. Dunkerton, "Nonlinear Propagation of Zonal Winds in an Atmosphere with Newtonian Cooling and Equatorial Wave Driving," *J. Atmos. Sci.* **48**, 236–263 (1991a).
25. R. A. Plumb, "The Interaction of Two Internal Waves with the Mean Flow: Implications of the Theory of the Quasi-Biennial Oscillation," *J. Atmos. Sci.* **34**, 1847–1858 (1977).
26. C. O. Hines, "Doppler Spread Parameterization of Gravity Wave Momentum Deposition in the Middle Atmosphere. Part 1. Basic Formulation," *J. Atmos. Terr. Phys.* **59**, 371–386 (1997).
27. C. O. Hines, "Doppler-Spread Parameterization of Gravity Wave Momentum Deposition in the Middle Atmosphere. Part 2. Broad and Quasi-Monochromatic Spectra, and Implementation," *J. Atmos. Terr. Phys.* **59**, 387–400 (1997).
28. J. R. Holton, *The Dynamic Meteorology of the Stratosphere and Mesosphere*, Meteorological Monographs, Vol. 15 (American Meteorological Society, Boston, 1975).
29. I. I. Mokhov and A. V. Eliseev, "Changes in the Characteristics of the Quasi-Biennial Oscillation of Zonal Wind and Temperature in the Equatorial Lower Stratosphere," *Izv. Akad. Nauk, Fiz. Atmos. Okeana* **34**, 327–336 (1998) [*Izv., Atmos. Ocean. Phys.* **34**, 291–299 (1998)].